Thin film CdS/CdTe and CdS/PbS photovoltaic solar cells

H. A. MOHAMED

Physics department, Faculty of Science, Sohag University, 82524 Sohag, Egypt
Department of Physics and Astronomy, College of Science, King Saud University, 11451 Riyadh, KSA

The current review article has focused on studying the effect of some losses such as the optical and recombination losses on the calculated short-circuit current density, cell efficiency and other cell parameters (such as: fill factor, open-circuit voltage, output power) of CdS/CdTe and CdS/PbS solar cells. The effect of the thickness of front electrode layer, the thickness of window layer (CdS), the thickness of absorber layer (CdTe or PbS), the width of space-charge region, the electron lifetime and the reflectivity from back contact were considered in this study. The optical losses which include the absorption in window layer and front electrode as well as the reflection at various interfaces recorded a value of 23-33% dependence on the thickness and optical properties of the window and front electrode layers. The front surface recombination losses are about 8% depend on the width of space charge region. The back surface recombination losses are mainly depending on the thickness of the absorber layer. The recombination losses in space charge region can be neglected at long electron lifetime of about 10^{-8} sec. The reflectivity of metallic back contact plays a significant role in enhancing the short current density particularly at low thickness of the absorber layer. The calculated efficiency of CdS/CdTe of 16.5 % agrees with the corresponding experimental values. The maximum efficiency of CdS/PbS of 6.1% is considered greater than those measured experimentally of this type of solar cells.

1. Introduction

At present, photovoltaic solar cells are one of the most important renewable energy sources[1-3]. Most modern solar cells are made from either crystalline silicon or thin film semiconductor material. Silicon cells are more efficient at converting sunlight to electricity, but generally have higher manufacturing costs[4]. Thin film materials typically have lower efficiencies, but can be simpler and less costly to manufacture. The best efficiency results reported for three of the more relevant thin film solar cell technologies are 18.3%, 20 % and 12.3 for CdS/CdTe, CdS/CIGS and a-Si, respectively [5]. The later types of solar cells have been fabricated based on mid-range band-gap semiconductors which absorb in the visible range of the solar spectrum.

CdTe is a material that exhibits a forbidden gap of 1.45 eV. Besides, its gap is direct and as a consequence its absorption coefficient is higher than 10^7 m^{-1} for energy larger than the forbidden gap. This means that only a few microns of material are enough to absorb all the light [6]. The absorber layer thickness for thin film CdTe solar cells is normally between 2 and 10 µm [7]. Thicker absorber layers are generally used to avoid pinholes reaching through to the window layer, which may lead to shorting from the back contact [8]. There are a number of experimental works that are mainly focused on reducing the absorber thickness CdTe layer. Gupta et al [9] reduced the CdTe thickness from 2.3 to 0.7 µm in CdS/CdTe solar cells without losing much efficiency. They obtained 11.8% cell efficiency with 0.87 µm CdTe compared to 13% obtained with standard 2.3 µm CdTe cells. Amin et al [10] used close-spaced sublimation method to grow CdTe layers of thickness 7-1.2 µm and obtained cell efficiencies of 15.3% and 11.5% , respectively. Recently, Paudel et al [11] prepared thin film CdS/CdTe cells with CdTe thickness from 0.25 µm to 2.1 µm. They obtained 8% efficiency with only 0.25 µm of CdTe and 11% efficiency with 0.5 µm.

The theoretical studies of CdS/CdTe solar cells recorded efficiency of 28-30 % [12, 13]. It is evident that there is a big difference between the experimental and theoretical values of the efficiency of CdS/CdTe. The main causes of efficiency loss are due to optical, electrical and recombination losses. Most of these theoretical works are mainly focused on the recombination and electrical losses [14-15]. Recently, L.A. Kosyachenko et al [16] studied the effect of optical losses on the efficiency of CdS/CdTe solar cells. The effect of both optical and recombination losses in CdS/CdTe solar cells are absent in the literature and this is maybe the reason of the big difference between theoretical and experimental results. The calculations have been carried out based on the optical losses (reflection and absorption) and recombination losses (font and back).

As mentioned above, photovoltaic devices usually exploit mid-range band-gap semiconductors which absorb in the visible range of the solar spectrum. However,

narrow band-gap semiconductors are of interest for photovoltaic (PV) solar energy conversion as they can absorb the "IR tail" of the solar spectrum, which is not absorbed by commonly used PV materials. The use of such absorbers in semiconductor sensitized solar cells allows the integration of low cost device configurations and broad spectral response, which may also be utilized in IR and near-IR (NIR) photodetectors [17]. Recently[18],material with narrow optical energy gap such as Lead sulfide (PbS), which has direct and narrow optical energy gap of 0.41 eV at 300 K, has been used as an absorber layer in thin film hetrostructure solar cells in order to absorb solar radiation near infrared region. The chemical bath deposition method was used to prepare thin film solar cell CdS/PbS with efficiency 1.37- 1.6 [18, 19]. The advantages of CdS/PbS solar cells are due to the unique properties of PbS, which can be summarized in some points such as: (1) PbS can absorb solar radiation near the infrared region of the solar spectrum, which is not absorbed by commonly used PV materials, (2) bulk-like PbS can be deposited by cheap, simple and energy-efficient methods involved in thin films deposition such as chemical bath deposition and electro-deposition [18, 20], (3) PbS is very sensitive to the grain size (much more than in classic semiconductors like Si), which makes it a good candidate for nanostructured devices [18], and finally (4) the effect of multiple exciton generation was recently discovered in nanostructures of PbS and similar semiconductor PbSe [21], which is very promising for solar cell applications. To our knowledge, the theoretical studies in this type of solar cell are absent in the literatures.

In this work, we try to get a match between experimental and theoretical results of CdS/CdTe solar cell as well as but fundamentals of the theoretical study of CdS/PbS solar cells. The effect of optical losses and recombination losses will be considered in this work. Moreover study the dependence of cell parameters such as the efficiency, fill factor, open-circuit voltage and the output power density on the thickness of TCO layer, the thickness of window layer, the thickness of absorber layer (PbS), the electron lifetime and the width of space-charge region.

2. Theoretical aspects of thin film photovoltaic solar cells

2.1 Structure of CdS/CdTe and CdS/PbS solar cells

The typical structure of photovoltaic thin film solar cells such as CdS/CdTe or CdS/PbS solar cells is shown in Fig.1.

This type of solar cells is composed of four layers:

1- Transparent conducting oxides layer (such as ITO) which is called front contact and has some required properties such as: highly transparent (more than 85% in visible region), highly conducting at room temperature (sheet resistance less than 10 Ω/square), and good adhesion to glass substrate [22];

2- CdS layer which is the so called window layer. This layer is used as n-type semiconductor. CdS has some required properties such as: relatively high transparency, not too thick to favors the absorption in the absorber layer, not too thin to avoid the short circuiting, relatively large conductivity to reduce the electrical solar cells losses and higher photoconductivity to not alter the solar cell spectral response [23].

3- The absorber (CdTe or PbS) which is made on top of CdS layer and is used as p-type semiconductor. CdTe has an ideal band-gap energy of ~1.5eV and high absorption coefficient (10^4 cm^{-1}) [24], a thin layer of CdTe is sufficient to absorb most of the incoming sunlight. While, PbS absorber has a narrow band-gap of 0.37-0.41 eV (300° K) [25] and then it can absorb the "IR tail" of the solar spectrum, which is not absorbed by commonly used PV materials.

4- Metal contact layer which is called the back contact and is deposited on top of the absorber layer. This layer must have high work function (>4.5 eV) to form ohmic contact with absorber layer and AU has been used in most cases. Besides, Ni-based contacts have also shown promising results [22].

Metal contact
Absorber

Fig.1. Schematics of a typical thin-film solar cell structure.

2.2 Transmission spectrum

According to the Fresnel equations, when the light is at near-normal incidence, the reflection coefficient (reflectivity) from the interface between two contacting materials is determined by their refractive indices n_1 and n_2:

$$R_f = \frac{(n_1 - n_2)^2}{(n_1 + n_2)^2} \tag{1}$$

In the case of electrically conductive materials, the refractive index contains an imaginary part and is written as $n^* = n - ik$, where n is the refractive index, and k is the extinction coefficient. The reflection coefficient from the interface is defined as the square of the modulus [($n^*_1 - n^*_2$)/($n^*_1 + n^*_2$)] [26] and has the form:

$$R = \frac{\left| n_1^* - n_2^* \right|^2}{\left| n_1^* + n_2^* \right|^2} = \frac{(n_1 - n_2)^2 + (k_1 - k_2)^2}{(n_1 + n_2)^2 + (k_1 + k_2)^2} \tag{2}$$

where n_1, n_2, k_1, k_2 are the refractive indices and extinction coefficients of the material one and two, respectively. In case of glass substrate $k=0$ and n values are calculated by Sellmeier dispersion equation and applied for quartz(SiO_2) [27]:

$$n^2 = 1 + \frac{a_1 \lambda^2}{\lambda^2 - \lambda_1^2} + \frac{a_2 \lambda^2}{\lambda^2 - \lambda_2^2} + \frac{a_3 \lambda^2}{\lambda^2 - \lambda_3^2} \qquad (3)$$

where $a_1 = 0.6962$, $a_2 = 0.4079$, $a_3 = 0.8974$, $\lambda_1 = 68$ nm, $\lambda_2 = 116$ nm, $\lambda_3 = 9896$ nm. The transmitted light that will reach the absorber layer after reflection at all interfaces of solar cell is calculated by the following formula:

$$T(\lambda) = (1 - R_{12})(1 - R_{23})(1 - R_{34})(1 - R_{45}) \qquad (4)$$

where R_{12}, R_{23}, R_{34}, R_{45} are the reflectivity of the interfaces air-glass, glass-TCO, TCO-window layer and window layer-absorberlayer, respectively.

When the absorption in TCO and window layers is taken into account, the transmitted light reaching the absorber layer is given by[28]:

$$T(\lambda) = (1 - R_{12})(1 - R_{23})(1 - R_{34})(1 - R_{45})(e^{-\alpha_1 d_1})(e^{-\alpha_2 d_2}) \qquad (5)$$

where α_1, α_2, d_1, d_2 is the absorption coefficient and thickness of ITO and CdS layers, respectively.

When the multi-reflections of L layers is taken into calculation, the Eq. (5) can be expressed in the following form:

$$T(\lambda) = 4 \frac{n_1 n_2}{(n_1 + n_2)^2} \prod_{j=2}^{L-1} \left(\frac{4 \frac{n_j n_{j+1}}{(n_j + n_{j+1})^2}}{1 - \frac{(n_j - n_{j-1})^2 (n_j - n_{j+1})^2}{(n_j + n_{j-1})^2 (n_j + n_{j+1})^2}} \right) \times \left(e^{-\alpha_1 d1} \right) \left(e^{-\alpha_2 d_2} \right) \qquad (6)$$

2.3 Quantum efficiency

The total internal quantum efficiency η_{int} of solar cell is the sum of the drift (η_{drift}) and diffusion (η_{dif}) components of quantum efficiency. This quantity is used in calculating the short-circuit current density. The drift component (η_{drf}), which takes into account recombination at the window layer-absorber layer interface (front recombination), is governed by the following expression [13]:

$$\eta_{drift} = \frac{1 + \frac{S}{D_n}\left(\alpha + \frac{2}{W}\frac{\varphi_0 - qv}{kT}\right)^{-1}}{1 + \frac{S}{D_n}\left(\frac{2}{W}\frac{\varphi_0 - qv}{kT}\right)^{-1}} - \exp(-\alpha W) \qquad (7)$$

where S is the recombination velocity at the heterojunction interface, D_n is the diffusion coefficient of electrons, α is the absorption coefficient of the absorber layer at a given wavelength, φ_0 is the barrier height at the semiconductor side, v is the applied voltage, q is the electron charge and k is the Boltzmann constant.

The dependence of width W of space-charge region (depletion layer) on the concentration of uncompensated acceptors ($N_a - N_d$) is given by

$$W = \sqrt{\frac{2\varepsilon\varepsilon_0(\varphi_0 - qv)}{q^2(N_a - N_d)}} \qquad (8)$$

where ε is the relative permittivity of the semiconductor and ε_0 is the permittivity of free space.

The diffusion component η_{dif} of the internal quantum efficiency, which takes into account recombination at the back surface of the solar cell, is given by the following expression[13]

$$\eta_{dif} = \frac{\alpha L_n}{\alpha^2 L_n^2 - 1} \exp(-\alpha W) \times$$

$$\left\{ \alpha L_n - \frac{\frac{S_b L_n}{D_n}\left[\cos\left(\frac{d-W}{L_n}\right) - \exp(-\alpha(d-W))\right] + \sinh\left(\frac{d-W}{L_n}\right) + \alpha L_n \exp(-\alpha(d-W))}{\frac{S_b L_n}{D_n}\sinh\left(\frac{d-W}{L_n}\right) + \cosh\left(\frac{d-W}{Ln}\right)} \right\} \qquad (9)$$

where $L_n = (\tau_n D_n)^{1/2}$ is the electron diffusion length, τ_n is electron lifetime, D_n is the electron diffusion coefficient, S_b is the recombination velocity at the back surface of the absorber layer and d its thickness.

2.4 Short-circuit current density

If Φ_i is the spectral radiation power density and $h\nu$ is the photon energy, the spectral density of the incident photon flux is $\Phi_i/h\nu$, and then the short-circuit current density J_{SC} is given by[13, 28]:

$$J_{SC}=q\sum_i T(\lambda)\frac{\phi_i(\lambda_i)}{h\nu_i}\eta(\lambda_i)\Delta\lambda_i \qquad (10)$$

where $T(\lambda)$ is the optical transmission and $\Delta\lambda_i$ is the interval between the two neighboring values λ_i. The calculations will be done for AM1.5 solar radiation using Tables ISO 9845-1:1992 (Standard ISO, 1992) [29].

2.5 Recombination losses in space-charge region (SCR)

The recombination losses in the space–charge region (SCR) can be studied, using the Hecht equation [30]:

$$\eta_H = \frac{\mu_p F(x,W)\tau_{p0}}{W}\left[1-\exp\left(-\frac{W-x}{\mu_p F(x,W)\tau_{p0}}\right)\right]+$$
$$\frac{\mu_n F(0,x)\tau_{n0}}{W}\left[1-\exp\left(-\frac{x}{\mu_n F(0,x)\tau_{n0}}\right)\right] \qquad (11)$$

where x is the coordinate s(x is measured from the CdS/CdTe or CdS/PbS interface), τ_{n0} and τ_{p0} are the lifetimes of electrons and holes in the SCR, respectively. τ_{n0} and τ_{p0} are related to the electron mobility μ_n and hole mobility μ_p according to the following equation:

$$\lambda_n = \mu_n F \tau_{n0} \qquad (12)$$

$$\lambda_p = \mu_p F \tau_{p0} \qquad (13)$$

where F is the strength of electric field.

In the Schottky diode, an electric field is not uniform in the space–charge region, but consideration of the nonuniformity is simplified, since the field strength decreases linearly with the x coordinate. In this case, the field strength F in the expressions (12) and (13) for λ_n and λ_p can be replaced by the average values of F in the sections(0, x) and(x, W) for electrons and holes, respectively [31]:

$$F(0,x) = \frac{\Phi_0 - ev}{eW}\left(2-\frac{x}{W}\right) \qquad (14)$$

$$F(x,W) = \frac{\Phi_0 - ev}{eW}\left(1-\frac{x}{W}\right) \qquad (15)$$

Then the charge collection efficiency in the SCR is determined by:

$$\eta_c = \int_0^W \eta_H(x)\alpha\exp(-\alpha x)dx \qquad (16)$$

2.6 Reflectivity from back contact

The effect of the reflectivity from the metallic back contact may reflect a significant impact to enhance the absorptivity in the absorber layer and then increase the photogenerated carriers particularly in a solar cell with a mirror back surface of the absorber layer. The following formula [32] can be used to measure theoretically the effect of reflectivity from the back contact on the internal quantum efficiency:

$$\eta_{int}(R)=\eta_{int}\left[1+R\times\exp(-\alpha d)\right] \qquad (17)$$

where R is the reflectivity from the back contact, α is the absorption coefficient of the absorber layer and d its thickness.

2.7 Cell parameters

To calculate the solar cell efficiency and output power density, many parameters such as; open-circuit voltage; maximum current density and maximum voltage must be firstly known. These parameters can be estimated from an illuminated J-V characteristic curve which can be presented in the form:

$$J(V)=J_d - J_{ph} \qquad (18)$$

where J_d is the dark current density and J_{ph} is the photocurrent density.

In most papers, the analytical description of J–V characteristics have been done using a semi-empirical formula for the dark current density in the so-called "ideal" solar cell which is described by the Shockley equation:

$$J_d(V)=J_S\left[\exp\left(\frac{qV}{kT}\right)-1\right] \qquad (19)$$

where J_s is the saturation current density equals the reverse current independent on the voltage V as qV is higher than a few kT. In this work, the J–V characteristics of CdS/CdTe and CdS/PbS heterostructure are governed by the generation- recombination Sah–Noyce–Shockley theory. The Sah-Noyce-Shockley theory supposes that the generation-recombination rate in the section x of the space-charge region is determined by expression [33]:

$$U(x,V)=\frac{n(x,V)P(x,V)-n_i^2}{\tau_{Po}[n(x,V)+n_1]+\tau_{no}[P(x,V)+P_1]} \qquad (20)$$

where τ_{no} and τ_{po} is the effective lifetime of electrons and holes in the depletion region, respectively, n_i is the intrinsic carrier concentration and the values n_1 and P_1 are determined by the energy spacing between the top of the valence band and the generation-recombination level E_t, i.e.

$$P_1 = N_v \exp(-(E_t/kT)) \qquad (21)$$

$$n_1 = N_c \exp(-(E_g - E_t)/kT) \qquad (22)$$

where N_c and N_v are the effective state densities in the conduction and valence bands, respectively and given by:

$$N_c = 2\left(\frac{m_n KT}{h^2}\right)^{3/2}, \; N_v = 2\left(\frac{m_p KT}{h^2}\right)^{3/2} \qquad (23)$$

In this equation, m_n and m_p are the effective masses of electrons and holes, respectively.

The values $n(x, V)$ and $P(x, V)$ in Eq. (20) are the carrier concentration in the conduction and valence bands and given by[34].

$$P(x,V) = N_c \exp\left[-\frac{\Delta\mu + \varphi(x,V)}{kT}\right] \qquad (24)$$

$$n(x,V) = N_v \exp\left[-\frac{E_g - \Delta\mu - \varphi(x,V) - qV}{kT}\right] \qquad (25)$$

where $\Delta\mu$ is the energy spacing between the Fermi level and the top of the valence band of the absorber layer and $\varphi(x, V)$ is the electron energy in the space charge region is given by:

$$\varphi(x,V) = (\varphi_0 - qV)\left(1 - \frac{x}{W}\right)^2 \qquad (26)$$

According to the Eqs.(20-26), the recombination-generation current are found by integration of $U(x, V)$ throughout the entire depletion layer [13]:

$$J_{gr} = q \int_0^W U(x,V)\, dx \qquad (27)$$

On the other hand, since in CdS/CdTe and CdS/PbS junctions the barrier for holes is higher than that for electrons, the electron component dominates the over-barrier current. Obviously, the electron flow current in analogous to that occurring in the p-n junction and one can write for the over-barrier current density [35]:

$$J_n == q\frac{n_p L_n}{\tau_n}\left[\exp\left(\frac{qV}{kT}\right) - 1\right] \qquad (28)$$

where n_p is the concentration of electrons in the bulk part of the p-type layer (CdTe or PbS), given by:

$$n_P = N_c \exp\left(-\frac{E_g - \Delta\mu}{kT}\right) \qquad (29)$$

Thus, according to the above-presented, the dark current density $J_d(V)$ is the sum of the generation-recombination and over-barrier components:

$$J_d(V) = J_{gr}(V) + J_n(V) \qquad (30)$$

The solar cell efficiency can be expressed by:

$$\eta = \frac{FF \times J_{SC} \times V_0}{P_{in}} \qquad (31)$$

where FF is the fill factor, V_0 is the open circuit voltage, P_{in} is the density of the total AM 1.5 solar radiation power (equals 96.3 mW/cm^2 [36]).

In the case of CdS/PbS cell, the efficiency is compared with the Shockley–Queisser limit that refers to the calculation of the maximum theoretical efficiency of a solar cell made from a single p-n junction. The dependence of this efficiency on the band gap energy (E_g) of the used absorber layer is given by the following expression [37]:

$$U(E_g) = \frac{E_g Q_S}{P_S} \qquad (32)$$

where Q_S is the number of absorbed photons (E < Eg) per unit area, per unit time and P_S is the solar power per unit area. This calculation assumed an idealized device so the practical limits are even smaller. The main assumptions are that all incident photons are captured, all above-band-gap photons are absorbed, complete thermalization occurs, the transport and collection of charges are lossless, and that only radiative or Auger recombination occurs.

The fill factor can be written as:

$$FF = \frac{P_m = J_m \times V_m}{J_{SC} \times V_0} \qquad (33)$$

where J_m and V_m are the maximum current density and voltage, respectively.

3. Results and discussions

3.1 Thin-film CdS/CdTe solar cells

The top curve in Fig. 2 represents the calculated transmission according to Eq.4. It can be noted that the reflection of all interfaces decreases the reached solar radiation to CdTe layer by about 9% in the average wavelength range of 500–850 nm. When the absorption losses are taken into calculations, it can be seen from this figure that the absorption in ITO and CdS layers leads to increase the losses by 18% in the average wavelength range of 500–800 nm at 100 nm thickness of each CdS and ITO layer. With further increase in ITO thickness (150–350 nm) more losses can be observed. Since the maximum losses (26%) are recorded at 350 nm thickness of ITO layer due to absorption. Then, the average of total optical losses is about 35% before the solar radiation reaches the absorber layer, particularly, at higher ITO thickness. It is expected that this loss ratio will increase with increasing

the value of CdS thickness because the thick layer leads to more absorption.
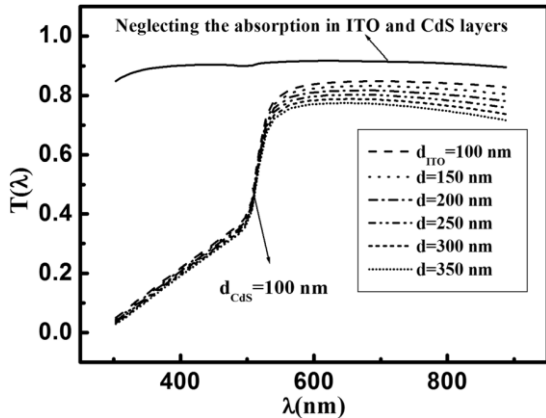

Fig.2. Calculated transmission (T) as a function of wavelength due to reflection losses (first curve) and reflection and absorption losses at different values of ITO thickness of CdS/CdTe solar cells [38]

The photoelectric quantum yield spectra (η) computed at different values of concentration of uncompensated acceptors (N_a-N_d) is shown in Fig.3. The present calculations of η are carried out under the following conditions; $S = 10^7$ cm/s, $\tau_n = 10^9$ s, $D_n = 25$ cm^2/s, $D_p = 2$ cm^2/s and φ_0-$qv = 1$ eV. It can be observed from the figure, with increasing the wavelength the photoelectric quantum yield increases and attains its maximum value at the photon energy close to the CdTe band-gap ($\lambda \sim 850$ nm). It can be concluded from Fig.3 that, the effect of surface recombination becomes strong at lower density of concentration of uncompensated acceptors (wide space-charge region).
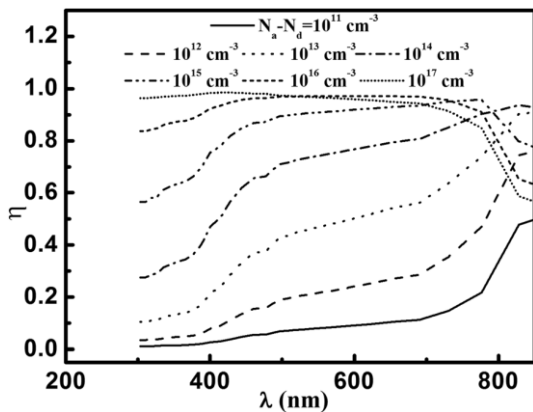
Fig. 3. The computed photoelectric quantum yield spectra (g) at different values of concentration of uncompensated acceptors (Na_Nd) of CdS/CdTe solar cells [38].

Fig. 4 shows the short-circuit current density J_{sc} of a CdTe-based solar cell as a function of ITO thickness when the reflection and absorption losses are taken into acount. In this case, the photoelectric quantum yield $\eta = 1$ and $d_{CdS} = 100$ nm. The first point (at zero x-axis) represents the effect of reflection losses only. At this point, J_{SC} is about 28.38 mA/cm^2. Comparing this value with the maximum

value $J_{SC}^0 = 31.24$ mA/cm^2, it is concluded that the reflection losses of the interfaces air-glass, glass- ITO, ITO-CdS, and CdS-CdTe lead to decrease in the maximum short-current density by 9%. When the absorption losses in both ITO and CdS layers are taken into account, the calculated J_{SC} decreases with further increase in ITO thickness and records 22.2 and 20.88mA/cm^2 at $d_{ITO} = 100$ and 350 nm, respectively. This indicates that the losses result from absorption ranged from 20% to 24%. Then, the total optical losses are about 29%−33%.
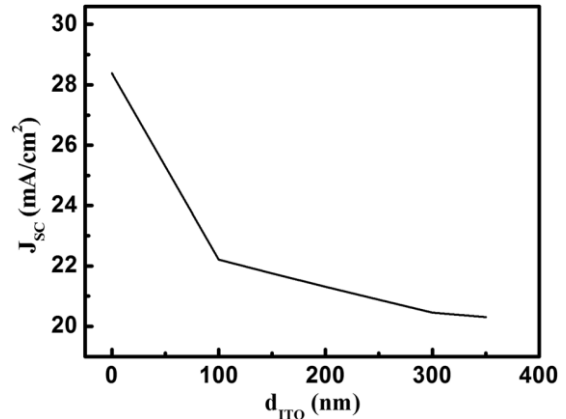

Fig. 4. Short-circuit current density J_{sc} of a CdTe-based solar cell as a function of ITO thickness under the optical losses [38].

The solar cell efficiency $\eta(\%)$ is calculated using V$_{OC}$ J$_{SC}$ FF/ P$_{in}$, where V_{oc} is the solar cell open-circuit voltage, FF is the fill factor and P_{in} is the input power. In these calculations V_{oc} is assumed to be 845 mV, FF is 75.5 % [22] and P_{in} is 100 mW/cm^2 for AM 1.5 global solar radiation. Fig. 5 shows the effect of optical and recombination losses on the efficiency of CdS/CdTe cell as a function of ITO thickness and different values of space-charge width. It is observed, the efficiency is in the range of 12-16 % for lowest width of space-charge region which corresponds to N_a-$N_d = 10^{16}$-10^{17} cm^{-3}. With decreasing the N_a-N_d values, the efficiency decreases dramatically and becomes less than 4% at N_a-$N_d = 10^{11}$ cm^{-3}. This result is considered in good agreement with other experimental studies [39-41]..
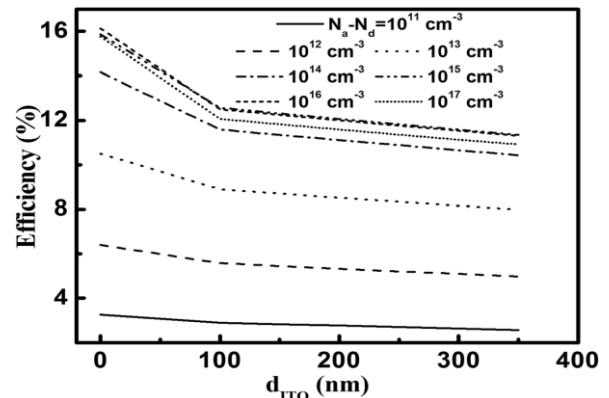
Fig. 5. Effect of the optical and recombination losses on the efficiency of a CdS/CdTe solar cell at various values of Na-Nd [38].

The drift and diffusion quantum yield spectra as a function of wavelength at different values of CdTe thickness are calculated from Eqs.(7-9) and plotted in Fig.6. In the present calculation, $(N_a\text{-}N_d)$ is taken as 10^{16} cm^{-3}.

It is noted that the drift component of quantum yield spectra (η_{drift}) slightly decreases with increasing the absorber thickness particularly at high wavelength. On the other hand, the diffusion component of quantum yield spectra (η_{dif}) increases with increasing the CdTe thickness indicating a remarkable dependence on the absorber thickness. Comparing Fig.6-a with Fig. 6-b, it is concluded that the main value of photoelectric quantum yield is coming from the drift component.
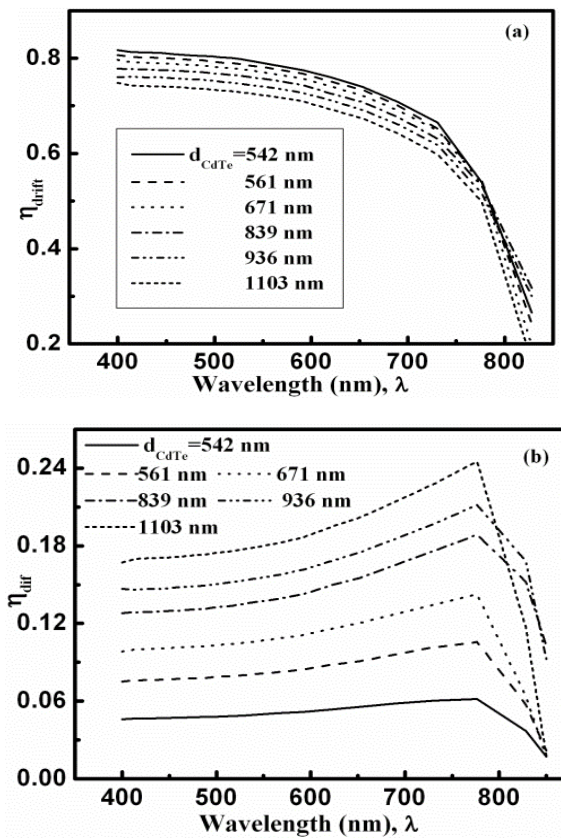
Fig.6. The drift (a) and diffusion (b) quantum yield spectra (η) are calculated at different values of CdTe thickness [42].

The effect of optical (reflection and absorption) and recombination (front and back recombination)losses on the calculated short-circuit current density (J_{SC}) at different thicknesses of CdTe absorber is shown in Fig.7. As shown in Fig.7-a, the reflection losses decrease the maximum value of current density (J^0_{SC} = 31.12 mA/cm^2) to 28.7 mA/cm^2 at CdTe thickness of 452 nm (i.e. the reflection losses=8%). Besides, the reflection and absorption losses lead to decrease J_{SC} by 15% at CdTe thickness of 452 nm.

Then, the optical losses (reflection and absorption) decrease the current density by a ratio of 23% and this ratio increases slightly to 24.5% when the thickness of absorber layer increases from 452 to 1103 nm indicating the small effect of CdTe thickness on the optical losses. Fig. 7-b shows the decreasing of drift component of current density with thickness which is due to decreasing the absorption coefficient with thickness. While increasing the diffusion component with thickness is due to increasing the absorbed photons as well as decreasing the surface recombination losses at the back surface of the CdTe layer. The effect of optical and recombination losses on the short-circuit current density can be seen in Fig.7-c. This figure indicates that the optical losses are in the range 23-24% corresponding to CdTe thickness 0.45-1.1 µm and the absorption losses contribute 15-16% of this ratio. While the recombination losses (front and back) are 28% at d_{CdTe}=0.45 µm and decrease to 23% at d_{CdTe}=1.1 µm indicating that the recombination losses have significant effect at thinner layers due to increasing the density of recombination centers.
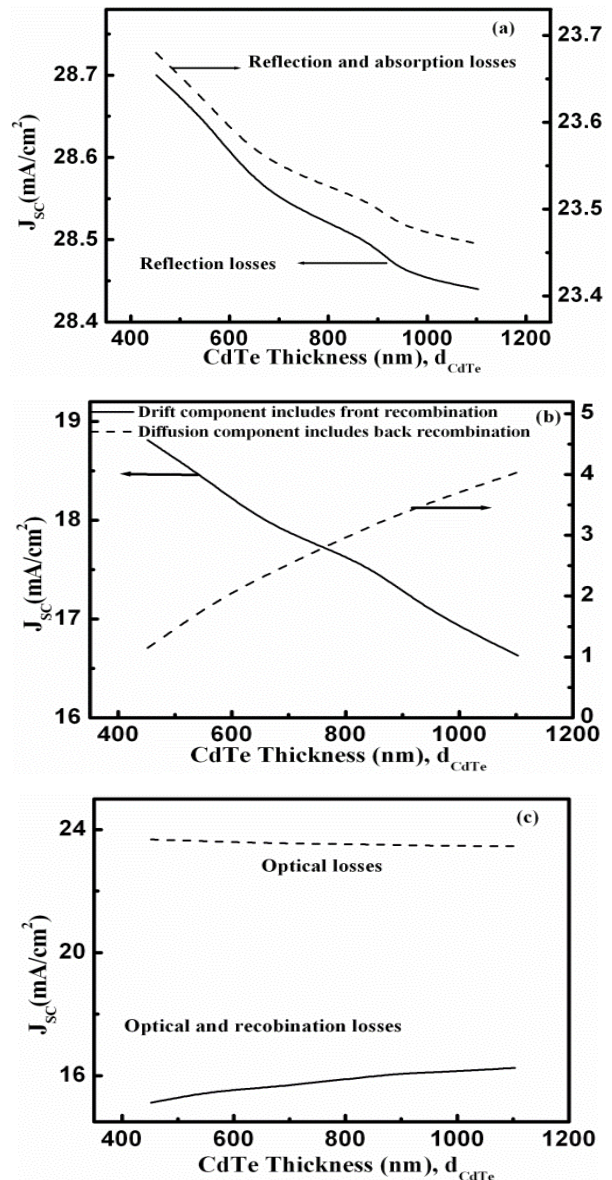
The dependence of cell efficiency on CdTe thickness and electron lifetime is shown in Fig.8. In these calculations V_{oc} is assumed to be 845 mV, *FF* is 75.5% [22] and P_{in} is 100 mW/cm^2 for AM 1.5 global solar radiation. It can be seen that the efficiency increases with increasing both the absorber thickness and electron lifetime and reaches the saturation case at higher values of electron lifetime. The maximum efficiency (10.5%) is observed at d_{CdTe}=1.1 µm and τ_n=10^{-9}-10^{-7} s.
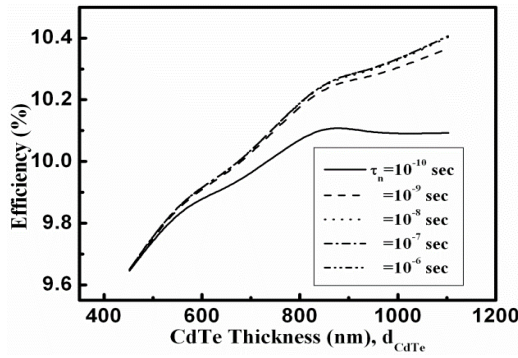
3.2 Thin-film CdS/PbS solar cells

Fig. 9 represents the dependence of η_{drift} on the width of space charge region (*W*). The calculations are carried out at S=10^7 cm/s (Fig.9–a) and at S=0 (Fig.9–b). The present width of space charge region 0.13–12 µm corresponds to the concentration of N_a-N_d in the range of 10^{17}–10^{13} cm^{-3}. Fig.9–a shows that η_{drift} decreases with increasing wavelength and decreasing the width of space charge region. The decreasing of η_{drift} with wavelength is due to decreasing of α with wavelength. With narrowing the barrier region from 12 µm to 0.13 µm (increasing N_a–N_d from 10^{13} cm^{-3} to 10^{17} cm^{-3}), the value of η_{drift} decreases due to a large portion of photons is absorbed outside the space-charge region and due to the small value of absorption coefficient of PbS material. When S=0 as shown in Fig.9–b, η_{drift} is close to 1 at lower wavelength and wide width of space charge region.
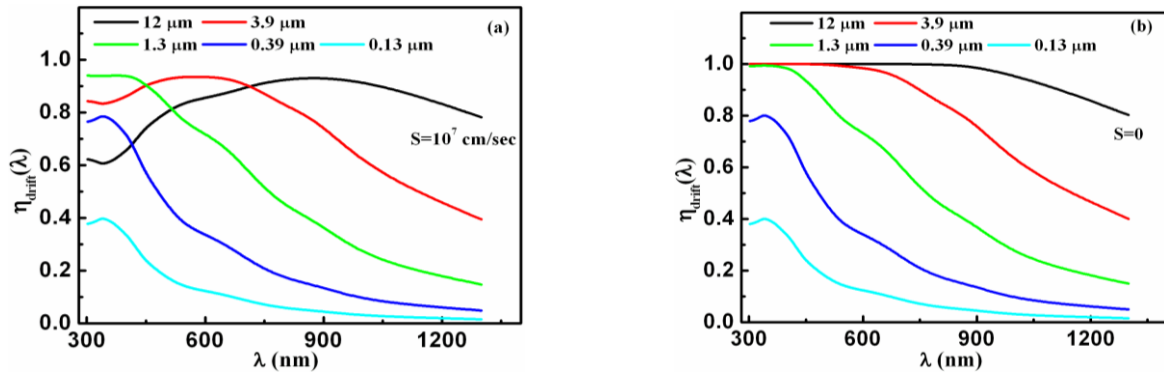
The second component (η_{dif}) of internal quantum efficiency as a function of wavelength at different values of PbS thickness and at *W*=0.39 µm is plotted in Fig.10. It is clear that the maximum η_{dif} is observed at thicker PbS and at S=0. Besides, the values of $\eta_{dif} < \eta_{drift}$ which means

that the contribution of diffusion component of quantum efficiency is small comparing with the contribution of drift component.
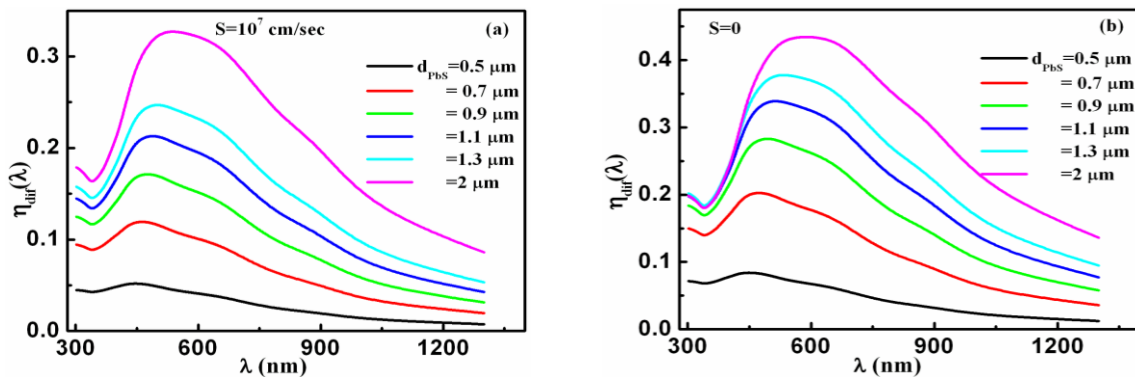
Fig.10. Diffusion component of internal quantum efficiency (η_{dif}) of CdS/PbS cell as a function of wavelength at different values of PbS thickness (d_{PbS}) at front surface recombination velocity $S=10^7$ cm/s (a) and $S=0$ (b) [43].

The dependence of short-circuit current density of CdS/PbS heterostructure on the thickness of the effective layer is calculated under the conditions of AM1.5 (96.3W/cm^2) solar irradiation and plotted in Fig.11. Calculations were made for the surface recombination velocities of S=10^7 cm/s and S=0. The width of space charge region is assumed to be 0.39 μm which corresponds to N_a–N_d=10^{16} cm^{-3}. In order to estimate the quantitative optical and recombination losses, we put $T(\lambda)$=1 and $\eta_{int}(\lambda)$=1 to obtain the maximum short-circuit current density of J_{SC}^0 =41 mA/cm^2 . At S=10^7 cm/s and when both the optical and recombination losses are taken into calculations, it is found that J_{SC}= 7.28 mA/cm^2 for d_{PbS}=0.5 μm and 13.2 mA/cm^2 for d_{PbS}=2 μm. This indicates that the optical and recombination losses are about 82% and 67% at d_{PbS}=0.5 μm and 2 μm, respectively. When the velocity of front surface recombination is reduced to zero, the values of J$_{SC}$ increase because the recombination losses decrease. In later case, the short-circuit current density records value of J_{SC}= 7.86 mA/cm^2 and 16 mA/cm^2 for d_{PbS}=0.5 μm and 2 μm, respectively. Then, the optical and recombination losses of this case are about 80% and 61%, respectively.

Fig. 12 shows *J–V* characteristics of thin film CdS/PbS solar cells at different thicknesses of PbS layer under the illumination condition of AM1.5 solar irradiation. It is clear from Fig.12–a that the illumination becomes more significant on CdS/PbS cell as the thickness of absorber is increasing. Fig.12-b compares between the dark and illuminated current of CdS/PbS solar cell at d_{PbS}=1300 nm. From this figure some important parameters such as V_0, V_m, J_m, *FF*, P_m and η are estimated and listed in table 1 as a function of PbS thickness.

Fig.12. J-V characteristic curve of CdS/PbS solar cell under illumination at various thicknesses of absorber layer (a) and the comparing between dark and illuminated current when the thickness of PbS is 1300 nm (b) [43].
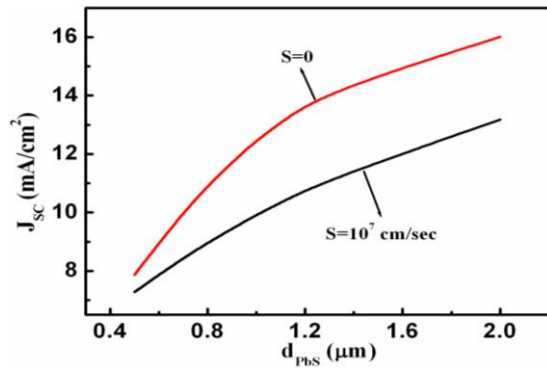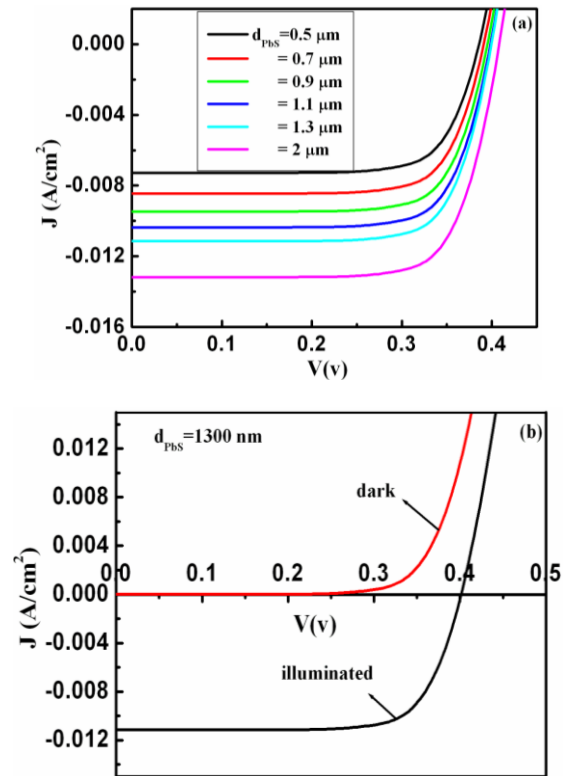

Fig. 11. Dependence of short-circuit current density (J_{SC}) on the thickness of absorber layer (d_{PbS}) at front surface recombination velocity S=10^7 cm/ s and S=0 cm/s of CdS/PbS cell [43].

Table 1. The maximum current density (J_m), maximum voltage (V_m), open circuit voltage (V_0), fill factor (FF), output power density (P_{out}) and efficiency (η)of thin film CdS/PbS solar cells at different values of thickness of the effective layer (PbS).

d_{PbS} (nm)	J_m (A/cm^2)	V_m (v)	V_0 (v)	FF (%)	P_{out} (mW/cm^2)	η (%)
500	0.0064	0.325	0.394	72.5	2.076	2.16
700	0.0071	0.336	0.398	70.9	2.38	2.47
900	0.0077	0.345	0.402	69.8	2.66	2.76
1100	0.0089	0.338	0.405	71.6	2.99	3.11
1300	0.0100	0.328	0.406	72.5	3.30	3.42

2000	0.0125	0.318	0.414	72.8	3.98	4.13

We can observe that, all these parameters expect *FF* increase with increasing the absorber thickness. The trend of the fill factor *FF* is weakly depending on the thickness of absorber layer. Firstly, it decreases slightly with thickness from 72% to 70 % and then starts to increase slightly with thickness to attain 72.8 at the highest thickness. Apart from the values of FF at PbS thickness range 700-900 nm, *FF* seems to be constant with average value of 72%. That indicate the capacity of the device to collect the charge carriers is approximately constant for various thickness of the absorber layer. The minimum cell efficiency of 2.16% is observed at d_{PbS}=0.5 μm, while the maximum efficiency is 4.13% is observed at d_{PbS}=2 μm. These values of efficiency are considered greater than the efficiency that estimated in some previous work [17, 19, 44].

The output power density of CdS/PbS solar cells as a function of applied voltage is shown in Fig.13 at different thicknesses of absorber layer. It can be seen that the maximum power is observed at applied voltage of 0.34 v and with increasing the thickness of absorber layer the power increases.
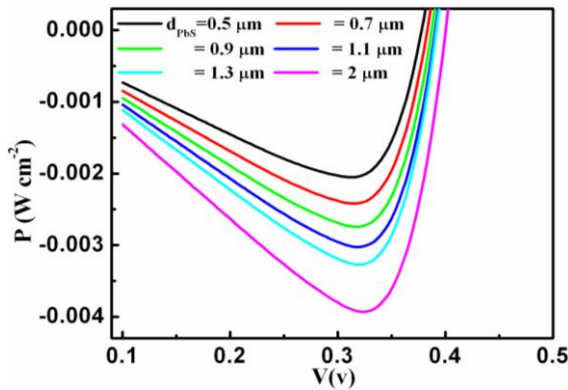

Fig.13. The output power density (P) as a function of applied voltage (V) at different thicknesses of the absorber layer of CdS/PbS solar cell [43].

The internal quantum efficiency is plotted in Fig.14 as a function of electron lifetime τ_n at different values of N_a-N_d. As shown in Fig.(14-a), when the space-charge region is wide (N_a-N_d is small) the effect of electron lifetime on the internal quantum efficiency can be neglected. The internal quantum efficiency decreases with decreasing both the electron lifetime and the width of space-charge region (increasing N_a-N_d) as shown in Fig. 14(b & c). The decrease of internal quantum efficiency with increasing N_a-N_d can be attributed to the larger portion of photons which are absorbed outside the space-charge region [14]. The decreasing of internal quantum efficiency with decreasing the electron lifetime is due to the recombination losses become more effective at low values

of lifetime. These results and the following results were carried at 3 μm thickness of the absorber layer (PbS).
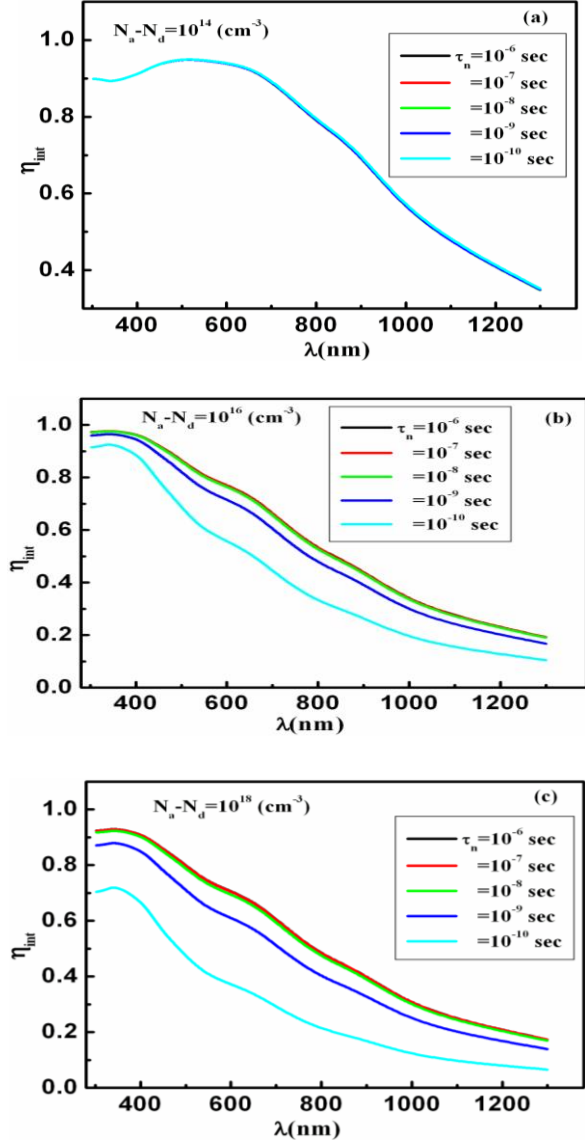

Fig.14. Internal spectral quantum efficiency η_{int} of CdS/PbS cell as a function of electron lifetime τ_n at different values of concentration of uncompensated acceptors of N_a-N_d=10^{14} cm^{-3} (a), N_a-N_d=10^{16} cm^{-3} (b) and N_a-N_d=10^{18} cm^{-3} (c) [45].

Fig. 15 represents the dependence of spectral internal and external quantum efficiency on the ratio of reflectivity from metallic back contact. The obtained results are carried out at τ_n=10^{-6} s and N_a-N_d=10^{16} cm^{-3}. As shown in this figure, both the internal external quantum and external quantum efficiency are increased with increasing the ratio of reflectivity from the metallic back contact. This result implies a significant effect of the back contact layer on the quantum efficiency and hence on the short-circuit current density.
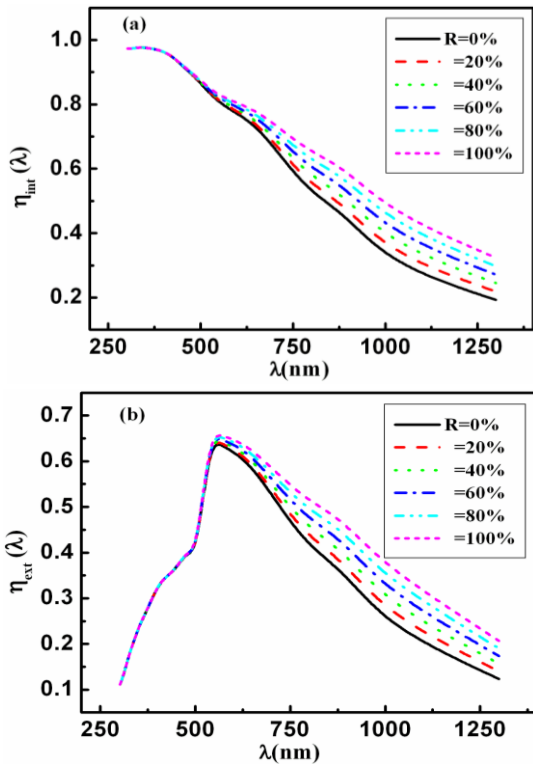
Fig.15. Internal spectral quantum efficiency η_{int} (a) and external spectral quantum efficiency η_{ex} (b) of CdS/PbS cell at different ratios of reflectivity (R%) from the back contact at $\tau_n=10^{-6}$ s and $N_a-N_d=10^{16}$ cm^{-3} [45].

Fig. 16 shows the charge collection efficiency (η_c) computed for different lifetimes and at fixed concentration of uncompensated acceptors (N_a-N_d) of 10^{15} cm^{-3}. It is clear that η_c increases with increase the value of x (which is measured from PbS side) and attains to saturation case when x is close to the width of space-charge region (W). Moreover, η_c increases with increasing the electron lifetime and its value is close to unity at $\tau_n=10^{-6}$ s. That indicates, the recombination losses in space-charge region can be ignored at high values of electron lifetime and this process has a considerable effect at low lifetime. The losses due to recombination are about 80 % at $x=0$, $\tau_n=10^{-10}$ s and much less losses (13%) are observed at $x=W$ at $\tau_n=10^{-10}$ s.
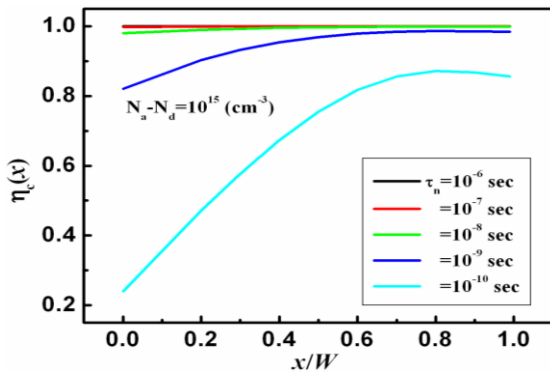

Fig.16. The coordinate dependences of the charge-collection efficiency η_c calculated for concentration of uncompensated acceptors of $N_a-N_d=10^{15}$ cm^{-3} and

different electron lifetimes τ_n of CdS/PbS cell [45].

The drift component of the short-circuit current J_{drift} is calculated from using the drift component of the internal quantum efficiency. It is known that the drift component of internal quantum efficient is mainly depending on the width of space-charge region (W). Therefore, the dependence of J_{drift} on N_a-N_d (or in W) is shown in Fig.(17-a). It is clear that J_{drift} decreases with increasing N_a-N_d (decreasing W). It is known that with increasing N_a-N_d, the electric filed becomes stronger and consequently the surface recombination becomes weaker resulting in an increase in J_{drift}. However in current work, J_{drift} decreases with N_a-N_d because a significant portion of the radiation is absorbed outside the space-charge region. On the other hand, Fig.(17-b) represents the dependence of diffusion component of the short-circuit current J_{dif} on electron lifetime τ_n at various values of N_a-N_d. It can be seen that J_{dif} increases with increasing N_a-N_d and τ_n. The maximum value of J_{dif} is about 14 mA/cm^2 at $\tau_n=10^{-6}$ s and $N_a-N_d=$ 10^{18} cm^{-3}. Also this figure refers to J_{dif} is approximately constant at lifetime longer than 10^{-8} s. It can be concluded that the back surface recombination has significant effect at short lifetime and wide space-charge region.
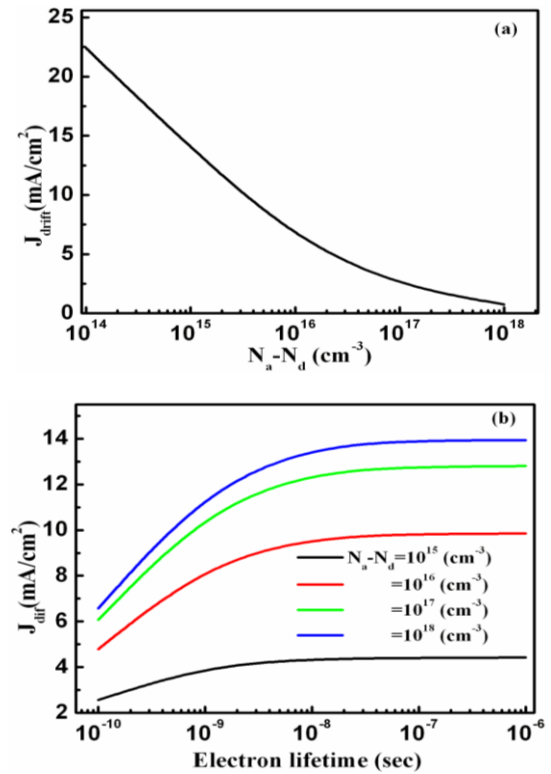

Fig.17. Dependence of drift component J_{drift} of current density on concentration of uncompensated acceptors N_a-N_d (a) and dependence of diffusion component J_{dif} of current density on electron lifetime at different concentrations of uncompensated acceptors(b) of CdS/PbS cell [45].

Under the illumination condition of AM1.5 solar irradiation, $J-V$ curve of CdS/PbS solar cell at different electron lifetimes and $N_a-N_d=10^{16}$ cm^{-3} is shown in Fig.18. It is clear that the $J-V$ curves are shifted down with

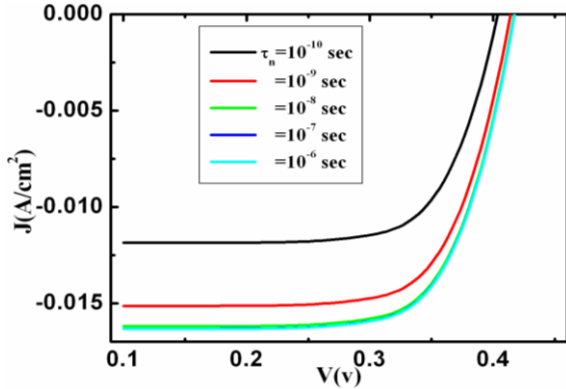increasing the electron lifetime indicating an increase in the photo-generated current density.

Fig.18. J-V characteristic of CdS/PbS solar cells at different values of electron lifetime under illumination condition of AM1.5 solar irradiation [45].

Fig. 19 shows *J-V* characteristic of CdS/PbS solar cells under illumination condition of AM1.5 solar irradiation at different ratios of reflectivity (*R%*) from the back contact at $\tau_n=10^{-6}$ s and N_a-$N_d=10^{16}$ cm^{-3}. It can be seen, increasing the reflectivity of back contact leads to more shift-down of all curves.
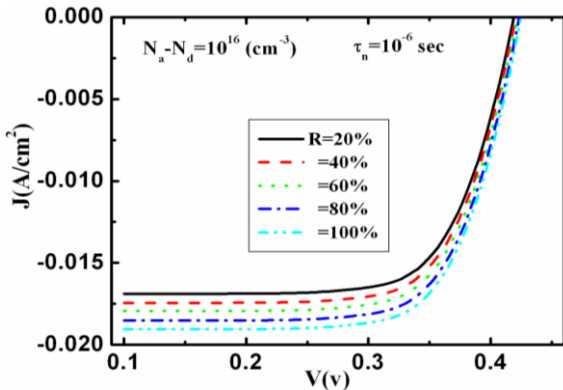

Fig.19. J-V characteristic of CdS/PbS solar cells under illumination condition of AM1.5 solar irradiation at different ratios of reflectivity (R%) from the back contact at $\tau_n=10^{-6}$ s and N_a-$N_d=10^{16}$ cm^{-3} [45].

The values of CdS/PbS cell efficiency (η), open-circuit voltage (V_0) and fill factor (*FF*) are estimated from Fig.18 and plotted in Fig.20 as a function of electron lifetime. Fig.(20-a) shows that the efficiency is increased with increasing the lifetime and the maximum efficiency of 5.17% is achieved at $\tau_n=10^{-6}$ s. From Fig.(20-b) we can notice that the minimum value of open-circuit voltage of 402 mV is observed at shorter lifetime (10^{-10} s). With further increase in carrier lifetime up to 10^{-8} s the value of V_0 increases up to 417 mV. Finally, V_0 approaches the saturation case at the lifetime range of 10^{-8} -10^{-6} s. Apart from $\tau_n=10^{-10}$ s, the fill factor (*FF*) seems to be constant (74%) for different values of lifetimes as shown in Fig. (20-c).

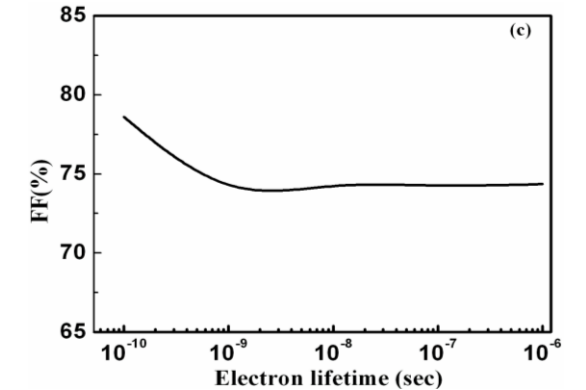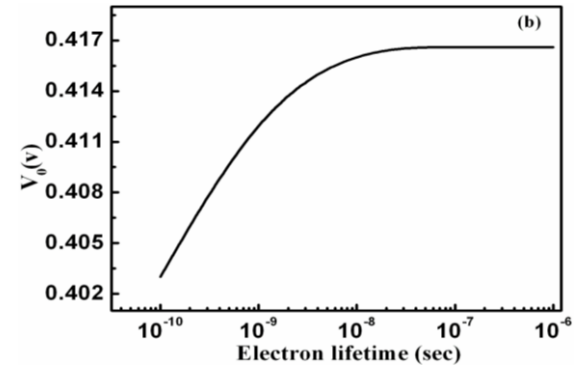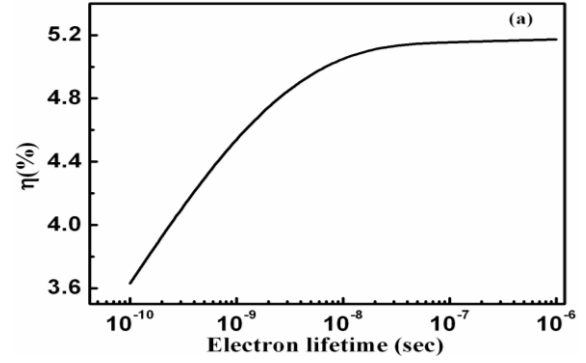*Fig.20. Dependence of the efficiency η(%) (a), open-circuit voltage V0 (b) and fill factor FF(%) (c) on electron lifetime of CdS/PbS solar cells [45].*

Moreover, comparing the current efficiency with Shockley–Queisser limit with applying the same assumption in Eq. (32) to PbS solar cells, the estimated upper limit reaches about 15% efficiency, which is almost three times the current highest efficiency achieved. The big difference between Shockley–Queisser and the current efficiency is mainly due to the optical and recombination losses.

When the effect of back contact is taken into calculations, the maximum current density, the maximum voltage, the open-circuit voltage and the cell efficiency are estimated from Fig.19 and listed in table 2. It is clear that all these parameters increase with increasing the ratio of reflectivity. The maximum efficiency of 6.1 % is achieved at $\tau_n=10^{-6}$ s and N_a-$N_d=10^{16}$ cm^{-3}.

Table 2. *The maximum current density (J_m), maximum voltage (V_m), open circuit voltage (V_0) and efficiency (η)of thin film CdS/PbS solar cells at different ratios of reflectivity from back contact at $\tau_n=10^{-6}$ s and $N_a-N_d=10^{16}$ cm^{-3}.*

$R(\%)$	V_0 (V)	V_m (V)	J_m (mA/cm^2)	η (100)
20	0.418	0.334	15.62	5.42
40	0.419	0.338	15.82	5.55
60	0.420	0.342	16.16	5.74
80	0.424	0.343	16.73	5.95
100	0.425	0.346	16.91	6.08

4. Conclusions

The efficiency of thin film photovoltaic solar cell with structures CdS/CdTe and CdS/PbS was studied theoretically based on the optical and recombination losses under certain parameters of the front electrode layer, window layer and absorber layer. In the case of CdS/CdTe cells, the obtained efficiency was about 16.5% based on the optical (reflection from all interfaces and absorption in ITO and CdS) and recombination (front and back surface) losses. When the thickness of the absorber layer reduced to1 μm, the efficiency of this type of solar cells recorded a value of 11 %. The efficiency of photovoltaic solar cell with structure CdS/PbS represented low efficiency comparing with CdS/CdTe cells. The efficiency of this type of solar cell can be enhanced under certain parameters of ITO layer, CdS layer, PbS layer, width of space-charge region, electron lifetime and reflectivity of back contact. The maximum efficiency of 5.17%, maximum open-circuit voltage of 417 mV and fill factor of 74% were performed at thickness of ITO =100 nm, thickness of CdS=100 nm, thickness of PbS= 3 μm, electron lifetime=10^{-6} s and uncompensated acceptors =10^{16} cm^{-3}. When the effect of back contact was considered, the efficiency increased and recorded a value of 6.1% when the back contact is completely reflective (100%).

Acknowledgment

References

[1] T. M. Razikov, C. S. Ferekides, D. Morel, E.Stefanakos, H.S.Ullal, H. M. Upadhyaya, Solar Energy **85**, 1580 (2011).

[2] A. Goetzberger, C. Hebling, Sol. Energy Mater. Sol. Cells **62**, 1 (2000).

[3] A. Goodrich, M. Woodhouse, PV Manufacturing Cost Analysis: Future Cost Reduction Opportunities, National Renewable Energy Laboratory (NREL), Golden, USA (2012).

[4] W. U. Huynh, J. J. Dittmer, A. P. Alivisatos, Science **295**, 2425 (2002).

[5] M.A. Green, K. Emery, Y. Hishikawa, W. Warta, E.D. Dunlop, Progress in Photovoltaics: Research and Applications **21**, 1 (2013).

[6] N. Romeo, A. Bosio, V. Canevari, A. Podesta, Sol. Energy **77** (2004) 795.

[7] E.W. Jones, V. Barrioz, S.J.C. Irvine, D. Lamb, Thin Solid Films **517**, 2226 (2009).

[8] A. Bosio, N. Romeo, S. Mazzamuto, V. Canevari, Prog. Cryst. Growth Ch. **52**, 247 (2006).

[9] A. Gupta, V. Parikh, A. D. Compaan, Sol. Energ. Mat. Sol. C. **90**, 2263 (2006).

[10] N. Amin, T. Isaka, A. Yamada, M. Konagai, Sol. Energ. Mat. Sol. C.**67**, 195 (2001).

[11] N.R. Paudel, K. A. Wieland, A. D. Compaan, Sol. Energ. Mat. Sol. C. **105**, 109 (2012).

[12] S. Sze, Physics of Semiconductor Devices, 2nd ed., Wiley, New York, 1981.

[13] L.A. Kosyachenko , A.I. Savchuk, E.V. Grushko, Thin Solid Films **517**, 2386 (2009).

[14] L.A. Kosyachenko, E.V. Grushko, V.V. Motushchuk, Solar Energy Materials & Solar Cells **90**, 2201 (2006).

[15] V.V. Brus, Solar Energy **86**, 786 (2012).

[16] L. A. Kosyachenko, E. V. Grushko, X. Mathew, Solar Energy Materials & Solar Cells **96**, 231 (2012).

[17] R. Gertman, A. Osherov, Y. Golan, I. V. Fisher, Thin Solid Films **550**, 149 (2014).

[18] J. H.Borja, Y. V. Vorobiev, R. Ramırez-Bon, Sol. Energy Mater. Sol. Cells **95**,1882 (2011).

[19] A. S. Obaid, M. A. Mahdi, Z. Hassan, M. Bououdin, Int. J. hydrogen energy. **38**, 807 (2013).

[20] M. G. Sandoval-Paz and R. Ramırez-Bon, Thin Solid Films **517**, 6747 (2009).

[21] R.J. Ellingson, M.C. Beard, J.C. Johnson, P. Yu, O.I. Micic, A.J. Nozik, A. Shabaev, A.L. Efros, Nano Letters **5**, 865 (2005).

[22] A. M. Acevedo, Solar Energy **80**, 675 (2006).

[23] A.Y. Jaber, S.N. Alamri, M.S. Aida, Thin Solid Films **520**, 3485 (2012).

[24] S. Singh, R. Kumar, K.N. Sood, Thin Solid Films **519**, 1078 (2010).

[25] D. K.Smith, J. M. Luther, O. E. Semonin, a. J. Nozik, M. C. Beard, ACS Nano **5**, 183 (2011).

[26] T.S. Moss, G.J. Burrel, D. Ellis, Semiconductor Opto-Electronics, Butterworth Publishers, New York, p. 12, 1973.

[27] S. O. Kasap, Optoelectronics and Photonics: Principles and Practice, Prentice Hall, New Jersey, p.45, 2000.

[28] H. A. Mohamed, Journal of Applied Physics **113**, 093105 (2013).

[29] Reference Solar Spectral Irradiance at the Ground at Different Receiving Conditions, Standard of International Organization for Standardization ISO 9845-1, 1992.

[30] K. Hecht, Z. Phys. **77,** 235 (1932).

[31] L. A. Kosyachenko, E. V. Grushko, V. V. Motushchuk, Sol. Energy Mater. Sol. Cells **90,** 2201 (2006).

[32] N.R. Paudel, K. A. Wieland, A. D. Compaan, Sol. Energy Mater. Sol. Cells **105,** 109 (2012).

[33] C. Sah, R. Noyce, W. Shokley, Proc. IRE **45,** 1228 (1957).

[34] L.A. Kosyachenko, V.M. Sklyarchuk, O.F. Sklyarchuk, V.A. Gnatyuk, Semicond. Sci.Technol. **22,** 911 (2007).

[35] S. Sze, Physics of Semiconductor Devices, 2nd ed., Wiley, New York, 1981.

[36] T. Toshifumi, S. Adachi, H. Nakanishi, K. Ohtsuka, 1993. Optical constants of Zn1xCdxTe ternary alloys: experiment and modeling. Jpn. Appl. Phys. 32, 3496–3501

[37] W. Shockley, H. J. Queisser, J. Appl. Phys **32**, 510 (1961).

[38] H.A. Mohamed, Journal of Applied Physics **113**, 093105 (2013)

[39] First Solar Inc. website at: /http://www.firstsolar.com/S.

[40] N. Amin, K. Sopian, M. Konagai , Solar Energy Materials & Solar Cells **91**, 202 (2007).

[41] A. Rios-Flores, O. Arés, J. M. Camacho, V. Rejon, J.L. Peña, Solar Energy **86**, 780 (2012).

[42] H. A. Mohamed, Canadian Journal of Physics **92**, 1350 (2014)

[43] H. A. Mohamed, Solar energy **108**, 360 (2014).

[44] A. S. Obaid, M. A. Mahdi, Z. Hassan, M .Bououdin, Superlattice. Microst. **52**, 816 (2012).

[45] H. A. Mohamed, Philosophical Magazine **94**, 3467 (2014).

_____

*Corresponding author:
hussein_abdelhafez2000@yahoo.com